U.P.B. Sci. Bull., Series D, Vol. 77, Iss. 4, 2015 ISSN 1454-2358

EFFECTS OF NAVIER SLIP AND WALL PERMEABILITY ON ENTROPY GENERATION IN UNSTEADY GENERALIZED COUETTE FLOW OF NANOFLUIDS WITH CONVECTIVE COOLING

Michael H MKWIZU[1], Oluwole D MAKINDE[2], Yaw NKANSAH-GYEKYE[3]

Present work investigates the effects of generalized Couette flow with convective cooling, Navier slip and permeable walls on entropy generation in an unsteady of water based nanofluids containing Copper (Cu) and Alumina (Al_2O_3) as nanoparticles. Both first and second laws of thermodynamics are applied to analyse the problem. The nonlinear governing equations of momentum and energy are solved numerically using a semi discretization finite difference method together with Runge-Kutta Fehlberg integration scheme. Graphical results on the effects of different parameter variations on velocity, temperature, skin friction, Nusselt number, entropy generation rate, and Bejan number are presented and discussed.

Keywords: Channel; Nanofluids; Couette flow; Entropy generation; permeability; Navier slip

1. Introduction

Thermodynamic irreversibility in the flow system provides information on the energy and power losses in the system. Minimization of entropy generation in the flow system enables the parametric optimization of the system operation. With the growing demand for efficient cooling systems, more effective coolants are required to keep the temperature of heat generating engines and engineering devices such as electronic components below safe limits. In recent time, the use of nanofluids has provided an innovative technique to enhance heat transfer.

The interest here is the study of the effect of heat transfer, permeable wall and Navier slip on entropy generation between two parallel plates, one of which is moving relative to the other and pressure gradient introduced known as generalized Couette flow which is motivated by several important problems in

[1] Mr.,School of Computational and Communication Science and Engineering, Nelson Mandela African Institution of Science and Technology,(NM-AIST) Tanzania, e-mails: mkwizum@nm-aist.ac.tz and Mr.,Dept of Biometry and Mathematics, Faculty of Science, Sokoine University of Agriculture, e-mails: mkwizumh@gmail.com
[2] Prof.,Faculty of Military Science, Stellenbosch University South Africa, e-mail: makinded@gmail.com
[3]PhD, School of Computational and Communication Science and Engineering, Nelson Mandela African Institution of Science and Technology,(NM-AIST), e-mails: mkwizum@nm- aist.ac.tz, yaw.nkansah-gyekye@nm- aist.ac.tz

engineering and industries. Nanotechnology has been widely used in engineering and industry since nanometer size materials possess unique physical and chemical properties. The addition of nanoscale particles into the conventional fluids like water, engine oil, ethylene glycol, etc., is known as nanofluid and was firstly introduced by Cho [1].

Hydromagnetic blood flow through a uniform channel with permeable walls covered by porous media of finite was done by Ramakrishnan and Shailendhra [2]. They found that the axial velocity of the fluid is reduced by porous parameter and Hartmann number. Theuri and Makinde [3] considered thermodynamic analysis of variable viscosity MHD unsteady generalized Couette flow with permeable walls. They found that the decrease in fluid viscosity increases Bejan number while an increase group parameter decreases Bejan number. As Reynolds number increases, Bejan number rises at the lower fixed plate and it falls at the upper moving plate.

The situation is reversed with increasing magnetic field. Oztop and Abu-Nada [4] considered natural convection in partially heated enclosures having different aspect ratio and filled with nanofluid. They found that the heat transfer was more pronounced at low aspect ratio and high volume fraction of nanoparticles. Wang and Mujumdar [5] presented a comprehensive review of heat transfer characteristics of nanofluids. Detail reports on convective transport in nanofluids can be found in Buongiorno [6], Tiwari and Das [7].

Meanwhile, in the nanofluids flows, the improvement of the heat transfer properties causes the reduction in entropy generation. The foundation of knowledge of entropy production goes back to Clausius and Kelvin's studies on the irreversible aspects of the second law of thermodynamics. Since then the theories based on these foundations have rapidly developed, see Bejan [8, 9].

However, the entropy production resulting from heat and mass transfer coupled with viscous dissipation in nanofluids has remained untreated by classical thermodynamics, which motivates many researchers to conduct analyses of fundamental and applied engineering problems based on second law analysis with respect to nanofluid. Based on the concept of efficient energy use and the minimal entropy generation principle, optimal designs of thermodynamic systems have been widely proposed by the thermodynamic second law [10]. It is possible to improve the efficiency and overall performance of all kinds of flow and thermal systems through entropy minimization techniques.

The analysis of energy utilization and entropy generation has become one of the primary objectives in designing a thermal system. Several studies have thoroughly dealt with conventional fluid flow irreversibility due to viscous effect and heat transfer by conduction [11, 12]. In the present study, we analyse the effects of convective cooling, Navier slip and permeable walls on entropy generation rate in unsteady generalized Couette flow channel of water base nanofluid.

2. Mathematical Model

Consider unsteady laminar flow of viscous incompressible nanofluids containing Copper (Cu) and Alumina (Al_2O_3) as nanoparticles through a permeable walls Couette flow channel. It is assumed that the fluid is injected uniformly into the channel at the lower plate while the uniform fluid suction occurs at the moving upper plate as depicted in Fig 1 below;

$$u = U\,,\ \ v = V\,,\ \ -k_{nf}\frac{\partial T}{\partial y} = h(T - T_w)$$

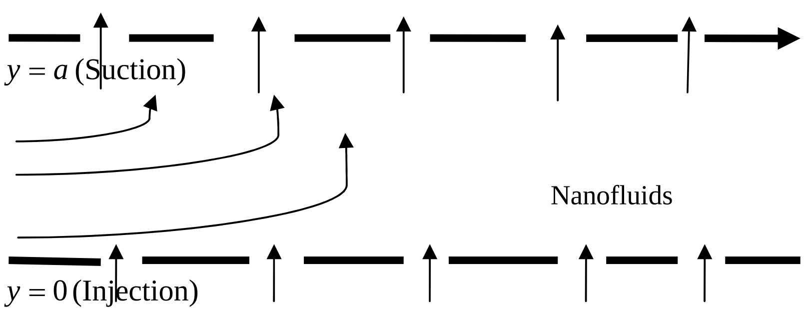

$$\mu_f \frac{\partial u}{\partial y} = -\beta u\,,\ \ v = V\,,\ T = T_w$$

Fig1: Schematic diagram of the problem under consideration

The governing equations for the nanofluids momentum and energy in one dimension with assumption above can be written as follows [7-9]

$$\frac{\partial u}{\partial \bar{t}} + V\frac{\partial u}{\partial y} = -\frac{1}{\rho_{nf}}\frac{\partial P}{\partial x} + \frac{\mu_{nf}}{\rho_{nf}}\frac{\partial^2 u}{\partial y^2}\,, \tag{1}$$

$$\frac{\partial T}{\partial \bar{t}} + V\frac{\partial T}{\partial y} = \alpha_{nf}\frac{\partial^2 T}{\partial y^2} + \frac{\alpha_{nf}\mu_{nf}}{k_{nf}}\left(\frac{\partial u}{\partial y}\right)^2, \tag{2}$$

where u is the nanofluid velocity in the x-direction, T is the temperature of the nanofluid, P is the nanofluid pressure, $\bar{t}$ is the time, a is the channel width, T_w is the lower stationary wall temperature, μ_{nf} is the dynamic viscosity of the nanofluid, k_{nf} is the nanofluid thermal conductivity, ρ_{nf} is the density of the nanofluid and α_{nf} is the thermal diffusivity of the nanofluid which are given by [3, 9]

$$\mu_{nf} = \frac{\mu_f}{(1-\varphi)^{2.5}}, \quad \rho_{nf} = (1-\varphi)\rho_f + \varphi\rho_s,$$
$$\alpha_{nf} = \frac{k_{nf}}{(\rho c_p)_{nf}}, \tau = \frac{(\rho c_p)_s}{(\rho c_p)_f}, \frac{k_{nf}}{k_f} = \frac{(k_s + 2k_f) - 2\varphi(k_f - k_s)}{(k_s + 2k_f) + \varphi(k_f - k_s)}, \tag{3}$$
$$(\rho c_p)_{nf} = (1-\varphi)(\rho c_p)_f + \varphi(\rho c_p)_s .$$

The nanoparticles volume fraction is represented by φ ($\varphi = 0$ correspond to a base fluid), ρ_f and ρ_s are the densities of the base fluid and the nanoparticle respectively, k_f and k_s are the thermal conductivities of the base fluid and the nanoparticles respectively, $(\rho c_p)_f$ and $(\rho c_p)_s$ are the heat capacitance of the base fluid and the nanoparticle respectively. It worth mentioning that the use of the above expression for k_{nf}, is restricted to spherical nanoparticles and does not account for other shapes of nanoparticles. Also, approximation has been employed to approximate the effective viscosity of the nanofluid μ_{nf} as viscosity of a base fluid μ_f containing dilute suspension of fine spherical particles. The initial and boundary conditions are given as follows:

$$u(y,0) = 0, \quad T(y,0) = T_w, \tag{4}$$

$$\mu_f \frac{\partial u}{\partial y}(0,\bar{t}) = -\beta u(0,\bar{t}), \quad T(0,\bar{t}) = T_w, \tag{5}$$

$$u(a,\bar{t}) = U, \; -k_{nf}\frac{\partial T}{\partial y}(a,\bar{t}) = h(T(a,\bar{t}) - T_w). \tag{6}$$

The table 1 below presents thermo physical properties of water, copper and alumina at the reference temperature.

Table 1

Thermophysical properties of the fluid phase (water) and nanoparticles [4, 7, 8, and 9]

Physical properties	**Fluid phase (water)**	**Cu**	**Al_2O_3**
c_p (J/kg K)	4179	385	765
ρ(kg/m^3)	997.1	8933	3970

The dimensionless variables and parameters are introduced as follows:

$$\left.\begin{array}{l} \theta = \dfrac{T - T_w}{T_w},\ W = \dfrac{u}{U},\ t = \dfrac{\bar{t}V}{a},\ \upsilon_f = \dfrac{\mu_f}{\rho_f},\ \overline{P} = \dfrac{Pa}{\mu_f U}, \\ A = -\dfrac{\partial \overline{P}}{\partial X},\ X = \dfrac{x}{a},\ \eta = \dfrac{y}{a},\ \Pr = \dfrac{\mu_f c_{pf}}{k_f},\ \ Ec = \dfrac{U^2}{c_{Pf} T_a}, \\ \tau = \dfrac{(\rho c_p)_s}{(\rho c_p)_f}, m = \dfrac{(k_s + 2k_f) + \varphi(k_f - k_s)}{(k_s + 2k_f) - 2\varphi(k_f - k_s)},\ \mathrm{Re} = \dfrac{Va}{\upsilon_f}, \alpha_f = \dfrac{k_f}{(\rho c_p)_f},\ f = \dfrac{\mu_f}{\beta a} \end{array}\right\} \quad (7)$$

The dimensionless governing equations together with the appropriate initial and boundary conditions can be written as:

$$\frac{\partial W}{\partial t} = \frac{A}{\mathrm{Re}\left(1 - \varphi + \varphi \rho_s / \rho_f\right)} + \frac{1}{\mathrm{Re}\left(1 - \varphi + \varphi \rho_s / \rho_f\right)(1-\varphi)^{2.5}} \frac{\partial^2 W}{\partial \eta^2} - \frac{\partial W}{\partial \eta} \quad (8)$$

$$\frac{\partial \theta}{\partial t} = \frac{1}{m \Pr \mathrm{Re}(1 - \varphi + \varphi\tau)} \frac{\partial^2 \theta}{\partial \eta^2} + \frac{Ec}{\mathrm{Re}(1-\varphi)^{2.5}(1 - \varphi + \varphi\tau)} \left(\frac{\partial W}{\partial \eta}\right)^2 - \frac{\partial \theta}{\partial \eta} \quad (9)$$

with initial and boundary conditions

$$W(\eta,0) = 0,\ \theta(\eta,0) = 0 \quad (10)$$

$$\frac{\partial W}{\partial \eta}(0,t) = -\frac{\beta a}{\mu_f} W(0.t),\ \theta(0,t) = 0 \quad (11)$$

$$W(1,t) = 1 \quad \frac{\partial \theta}{\partial \eta}(1,t) = -mBi\,\theta(1,t) \quad (12)$$

where $\Pr$ is the Prandtl number, Ec is the Eckert number, Re is the Reynolds number, A is the pressure gradient parameter, β is the coefficient of sliding fraction and *f* is slip parameter. Other physical quantities of practical interest in this problem are the skin friction coefficient C_f and the local Nusselt number Nu which are defined as

$$C_f = \frac{a\tau_w}{\mu_f U},\ \ Nu = \frac{aq_w}{k_f T_w}, \quad (13)$$

where τ_w is the wall shear stress and q_w is the heat flux at the channel walls given by

$$\tau_w = -\mu_{nf} \left.\frac{\partial u}{\partial y}\right|_{y=a},\ \ q_w = -k_{nf} \left.\frac{\partial T}{\partial y}\right|_{y=a} \quad (14)$$

Substituting equations (14) into (13) and using dimensionless variables, we obtain

$$\left.C_f = -\frac{1}{(1-\varphi)^{2.5}} \frac{\partial W}{\partial \eta},\ Nu = -\frac{1}{m}\frac{\partial \theta}{\partial \eta}\right\} \text{at } \eta = 1. \quad (15)$$

3. Entropy Analysis

The second law of thermodynamics is an important tool to scrutinize the irreversibility effects due to flow and heat transfer. Thermodynamic irreversibility is closely related to entropy production. Convection process involving channel flow of nanofluids is inherently irreversible due to the exchange of energy and momentum, within the nanofluid and at solid boundaries. Following Woods [10], the local volumetric rate of entropy generation is given by

$$S''' = \frac{k_{nf}}{T_w^{\,2}}\left(\frac{\partial T}{\partial y}\right)^2 + \frac{\mu_{nf}}{T_w}\left(\frac{\partial u}{\partial y}\right)^2 \tag{16}$$

The first term in equation (16) is the entropy generation due to heat transfer while the second term is the entropy generation due to nanofluid friction. Using dimensionless variables from equation (7), we express the entropy generation number in dimensionless form as,

$$Ns = \frac{a^2 S'''}{k_f} = \frac{1}{m}\left(\frac{\partial \theta}{\partial \eta}\right)^2 + \frac{Br}{(1-\varphi)^{2.5}}\left(\frac{\partial W}{\partial \eta}\right)^2 \tag{17}$$

Where $Br = Ec\Pr$ is the Brinkman number, the Bejan number Be is define as

$$Be = \frac{N_1}{Ns} = \frac{1}{1+\Phi} \tag{18}$$

Where, $N_s = N_1 + N_2$. $N_1 = \frac{1}{m}\left(\frac{\partial \theta}{\partial \eta}\right)^2$ (The entropy generation due to heat transfer), $N_2 = \frac{Br}{(1-\varphi)^{2.5}}\left(\frac{\partial W}{\partial \eta}\right)^2$ (The entropy generation due to fluid friction)

The irreversibility distribution ratio is define as $\Phi = N_2/N_1$. Heat transfer irreversibility dominates for $0 \le \Phi < 1$ and fluid friction irreversibility dominates when $\Phi > 1$. The contribution of both irreversibilities to entropy generation is equal when $\Phi = 1$.Equation (18) shows that the Bejan number ranges from 0 to 1. The zero value of the Bejan number corresponds to the limit where the irreversibility is dominated by the effect of fluid friction while one value of Bejan number is the limit where the irreversibility due to heat transfer dominates the flow system. The contribution of both heat transfer and fluid friction to irreversibility are the same when $Be = 0.5$.

4. Numerical Procedure

Using a semi-discretization finite difference method, the nonlinear initial boundary value problem (IBVP) in equations (8)-(12) can be solved numerically. We partition the spatial interval into equal parts and define grid size and grid points. The first and second spatial derivatives in equation (8) and equation (9) are approximated with second-order central finite differences.

$$\frac{dW_i}{dt} = \frac{A}{\operatorname{Re}\,(1-\varphi+\varphi\rho_s/\rho_f)} + \frac{(W_{i+1}-2W_i+W_{i-1})}{\operatorname{Re}\,(1-\varphi+\varphi\rho_s/\rho_f)(1-\varphi)^{2.5}(\Delta\eta)^2} - \frac{W_{i+1}-W_{i-1}}{2\Delta\eta} \tag{19}$$

$$\frac{d\theta_i}{dt} = \frac{(\theta_{i+1}-2\theta_i+\theta_{i-1})}{m\Pr\operatorname{Re}\,(1-\varphi+\varphi\tau)(\Delta\eta)^2} + \frac{Ec}{\operatorname{Re}\,(1-\varphi+\varphi\tau)(1-\varphi)^{2.5}}\left(\frac{W_{i+1}-W_{i-1}}{2\Delta\eta}\right)^2 - \frac{\theta_{i+1}-\theta_{i-1}}{2\Delta\eta} \tag{20}$$

with initial conditions and boundary conditions

$$W_i(0) = \theta_i(0) = 0,\ 1 \le i \le N+1 \tag{21}$$

$$W_1 = \frac{-fW_2}{\Delta\eta - f},\ \theta_1 = 0, W_{N+1} = 1,\quad \theta_{N+1} = \theta_N(1 - mBi\Delta\eta) \tag{22}$$

Considering equations (19)-(22) we can see that, they are first order ordinary differential equations with known initial conditions. So they can be easily solved iteratively using Runge-Kutta Fehlberg integration technique implemented on computer using Matlab. The skin-friction coefficient and the Nusselt number in equation (15) are also worked out and their numerical results are presented.

5. Results and Discussions

For understanding the dynamics of this physical problem, Figs 2-23 shows the numerical computations for the representative velocity field, temperature field, skin friction, Nusselt number, entropy generation rate and Bejan number. Some arbitrary chosen specific values to various thermophysical parameters controlling the flow system have been assigned. The detailed discussion and graphical representation are reported in this section.

5.1 Effects of parameter variation on velocity profiles

It is noted that, the velocity increases with time for a given set of parameter values until a steady state profile is achieved as shown in Fig 2. Fig 3 shows an interesting observation that, alumina-water nanofluid tends to flow faster than copper-water nanofluids. This result may be due to the high density of copper nanoparticle as compared to alumina nanoparticle. An increase in nanoparticles volume fraction causes a slight decrease in the velocity profile see Fig 4. This may be due to the density, the dynamic viscosity of the nanofluid, slip condition, suction and injection of the fluid. Looking to Fig 5, it can be noted that the nanofluid velocity increases with an increase in pressure gradient. The opposite effect is observed in Fig 6 where increasing Reynolds number causes a decrease in velocity profile. This happens because the viscous force increases within the flow system.

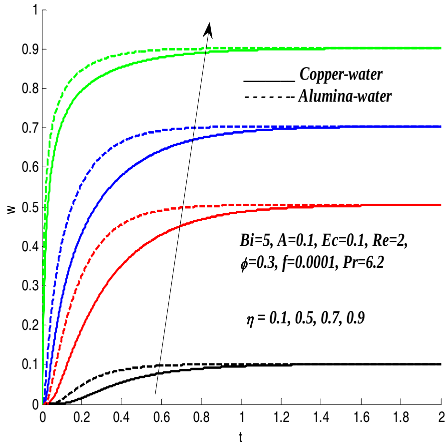

Fig 2: Nanofluids velocity profile with profiles with increasing time

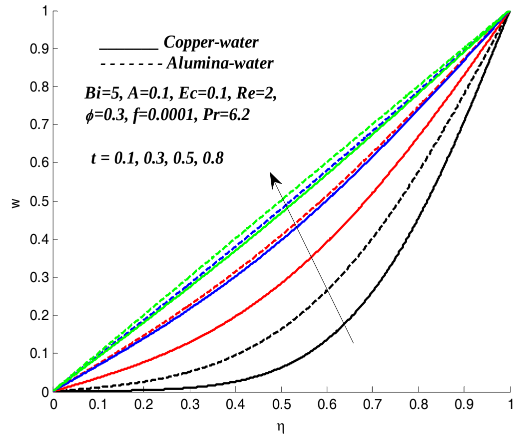

Fig 3: Nanofluids velocity with increasing time

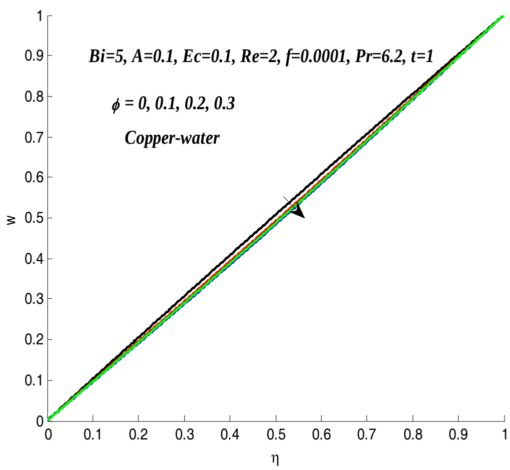

Fig 4: Nanofluid velocity profiles with increasing ϕ

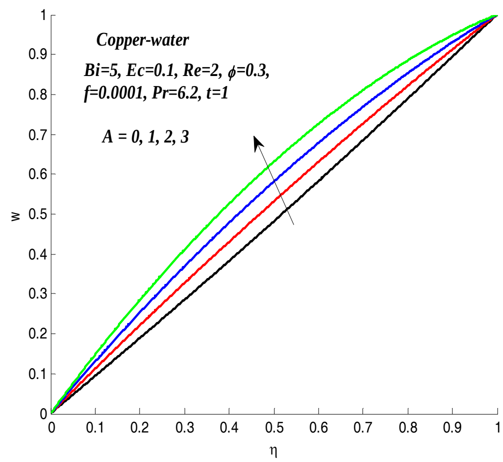

Fig 5: Nanofluid velocity profiles with increasing A

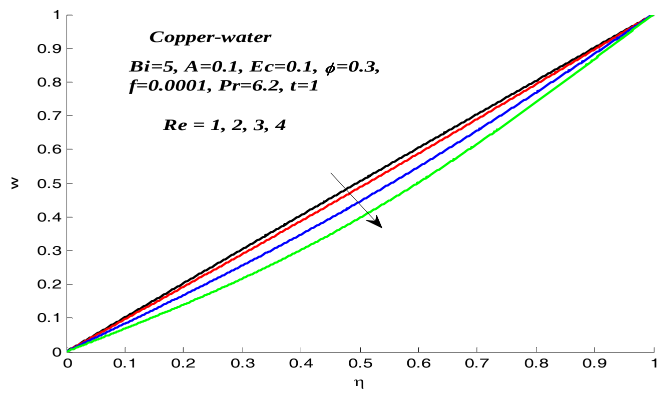

Fig 6: Nanofluid velocity profiles with increasing *Re*

5.2 Effects of parameter variation on temperature profiles

The transient effects on the nanofluids temperature profiles are clearly revealed in Figs 7-12. From Fig 7 it is noted that the temperature increases with time near the lower wall it then decreases toward the upper moving wall for a given set of parameter values until a corresponding steady state profile is achieved. This behaviour may be attributed by the slip condition and injection at the lower wall, suction and moving upper wall. Interestingly, the temperature of Cu-water nanofluid rises higher than that of Al_2O_3-water nanofluids as shown in Fig 8. Moreover, with increase in time the alternating temperature is observed. The temperature profile attains its maximum value at the upper wall and minimum value at the lower wall. Figs 9-12 illustrate the effects of parameter variation on the temperature profiles with Cu-water as the working nanofluid. It is observed that the temperature profile increases with an increase in the nanoparticles volume fraction as shown in Fig 9. Similar trend of increase in temperature is noticed with increase in slip parameter, this behaviour may be attributed by slippery at the walls as shown in Fig 10. Opposite behaviour is observed in Fig 11 that, nanofluid temperature falls with an increase in Biot number. It is noted that with an increase in Eckert number the temperature profile rises as shown in Fig 12. This increase in temperature may be attributed by viscous dissipation.

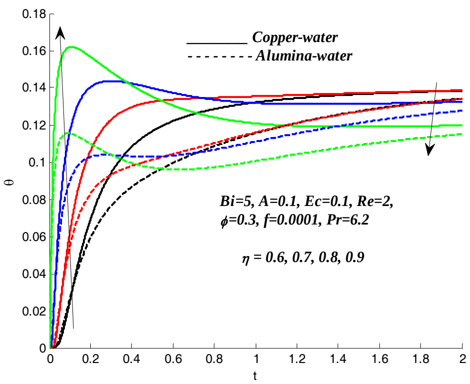

Fig 7: Nanofluids temperature profiles with increasing time

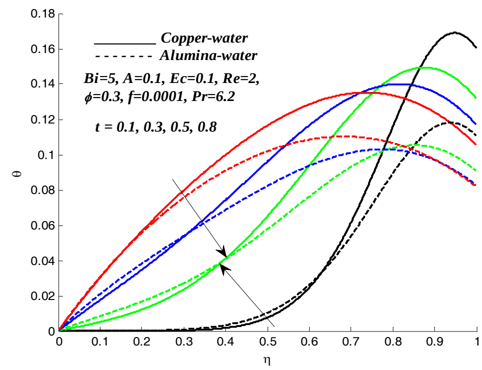

Fig 8: Nanofluids temperature profiles with increasing time

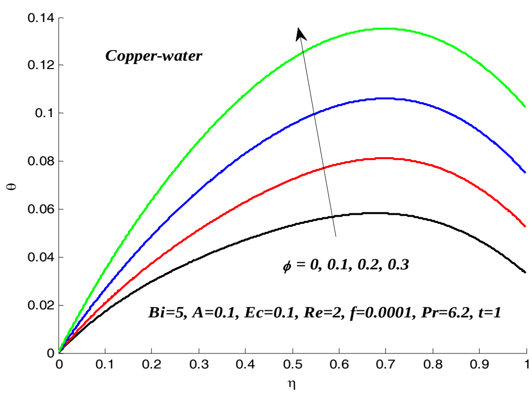

Fig 9: Nanofluid temperature profiles profiles with increasing ϕ

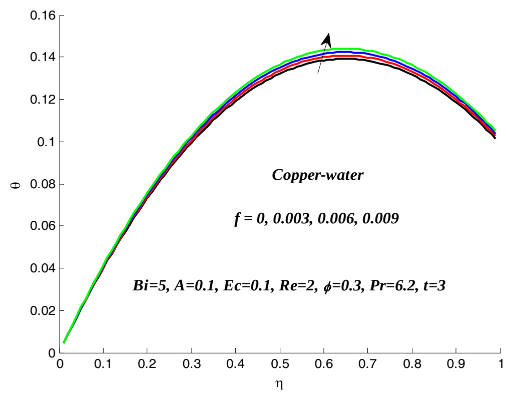

Fig 10: Nanofluid temperature with increasing f

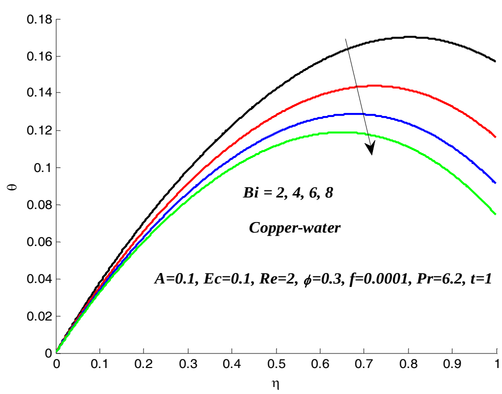

Fig 11: Nanofluid temperature profiles profiles with increasing *Bi*

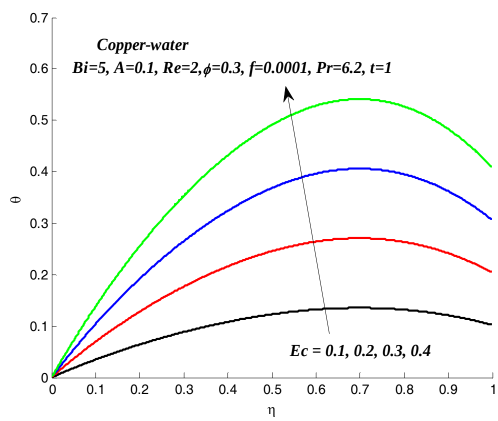

Fig12: Nanofluid temperature with increasing *Ec*

5.3 Skin friction and Nusselt number

Fig 13 and Fig 14 illustrate the effects of parameter variation on skin friction and Nusselt number using Cu-water as a working nanofluid. In fig 13, it is observed that the skin friction increases with an increase in nanoparticles volume fraction. This may be due to movement of the upper wall, injection at the lower wall and suction at the upper wall. It is also noted that the skin friction is small at the injection wall and increase toward the suction wall. Moreover interesting result is observed, that the skin friction increases with an increase in Reynolds number and the slight increase is observed when increase in slip parameter but decrease with increase in pressure gradient.

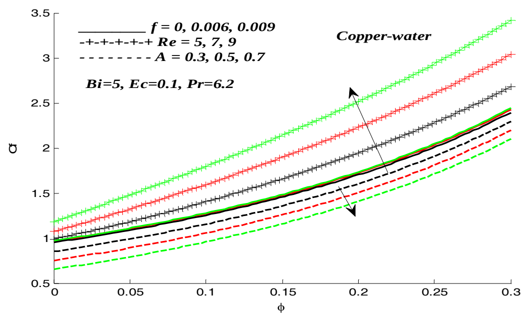

Fig 13: Skin friction with increasing ϕ, A, Re and f

Meanwhile, the Nusselt number increases with an increase in nanoparticles volume fraction, Reynolds number and slip parameter but decrease with an increase in pressure gradient as illustrated in Fig 14. This may be attributed by Couette flow at the upper wall, injection and suction.

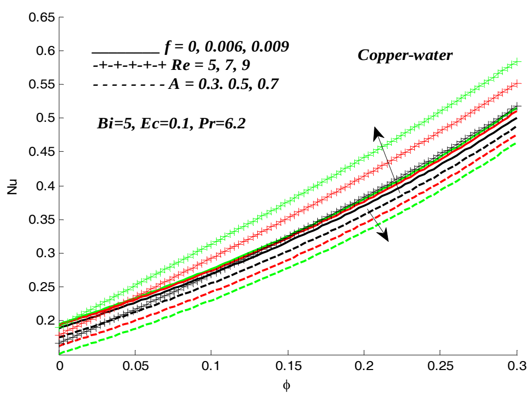

Fig 14: Nusselt number with increasing ϕ, A, Re and f

5.4 Effects of parameter variation on entropy generation rate

Fig 15 shows that the entropy generation rate increases with time at the lower wall and decrease with time across the upper wall. This behaviour may be due to slip and injection at the lower wall, and Couette flow together with suction. The entropy generated by Al_2O_3-water nanofluid is higher near the lower wall compared with that generated by Cu-water nanofluid and reverse as it approaches the upper wall. A rise in an entropy generation rate is observed at the walls with an increase in nanoparticles volume fraction as illustrated in Fig 16. Similar observation is noted in Fig 17 with an increase in slip condition. Fig 18 shows that the entropy generation rate decreases at the lower wall with an increase in Biot number and reverse its trend as it approaches the upper wall.

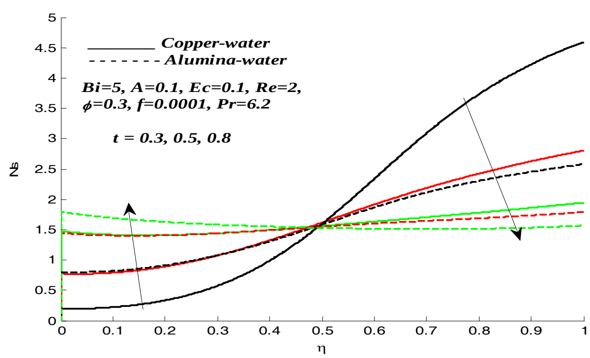

Fig 15: Entropy generation rate with rate increasing time

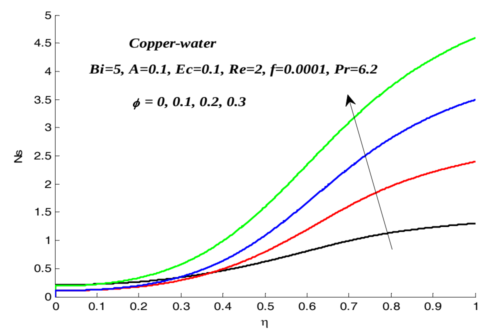

Fig 16: Entropy generation with increasing ϕ

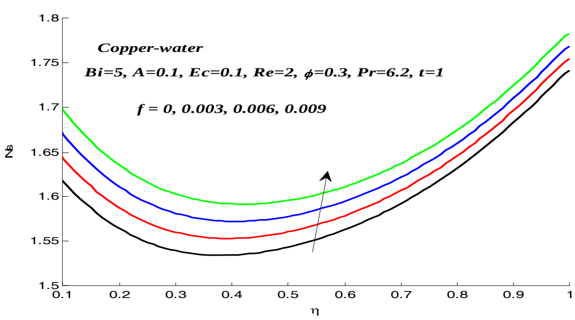

Fig 17: Entropy generation rate with increasing *f*

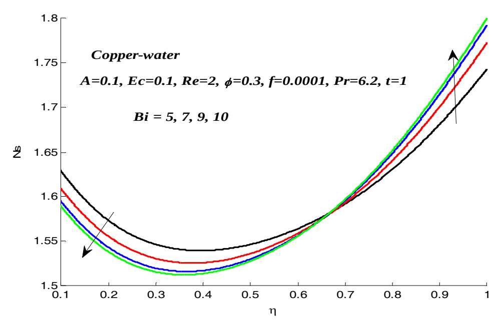

Fig 18: Entropy generation rate with increasing *Bi*

5.5 Effects of parameter variation on Bejan number

Fig 19 illustrates the transient effect on the Bejan number across the channel. The Bejan number increase with time near the channel lower walls but the slight decreases is noted at the channel centreline. This can be because of rise in the dominant effect of fluid friction irreversibility within the channel centreline region, the heat transfer irreversibility at the channel walls, injection, suction, slip condition and the Couette flow. The Bejan number produced by Cu-water nanofluid seems to be higher than that of Al_2O_3-water nanofluid. Fig 20 shows an increase in the Bejan number at the walls with an increase in nanoparticles volume fraction. This implies that increase in nanoparticles volume fraction causes domination effects of fluid friction irreversibility. Furthermore, it is observed in Fig 21 that, the Bejan number decreases at lower wall and at the centreline of the channel, but increases as it approaches the upper wall. Different trend is observed in Fig 22, when increasing Eckert number the Bejan number increases in both walls. Meanwhile, the decrease in Bejan number is observed at the lower wall and centre but increase as it approaches the upper wall with an increase in pressure gradient as shown in Fig 23. Generally, this behaviour may be attributed by slip condition, injection, suction, convective cooling and upper moving wall.

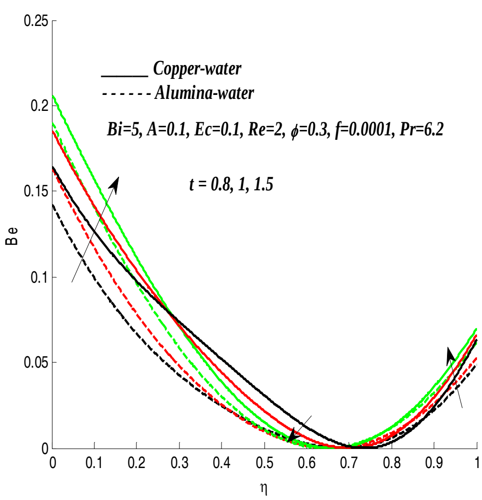

Fig 19: Bejan number with increasing time

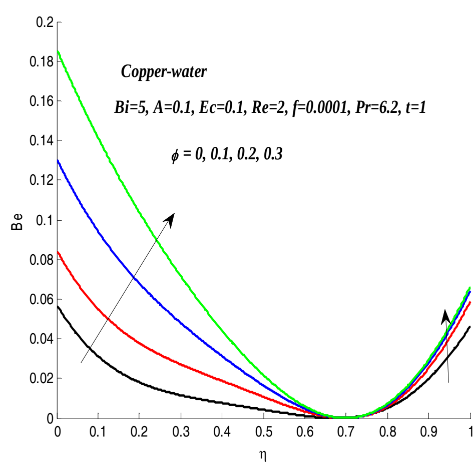

Fig 20: Bejan number with increasing ϕ

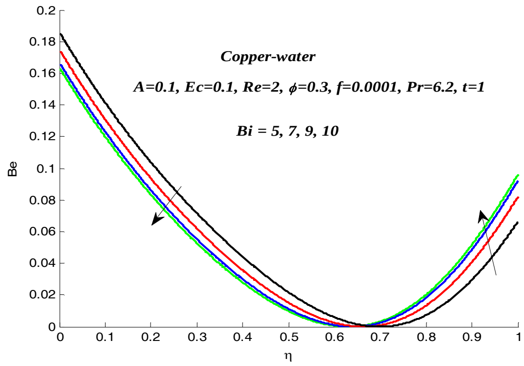

Fig 21: Bejan number with increasing *Bi*

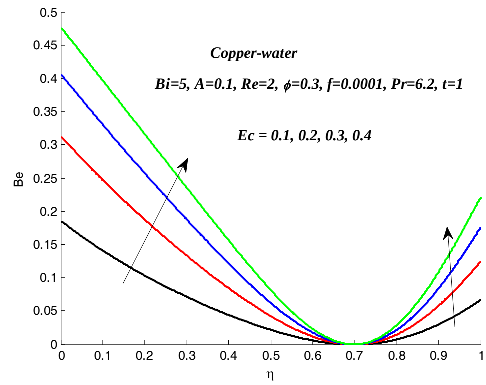

Fig 22: Bejan number with increasing *Ec*

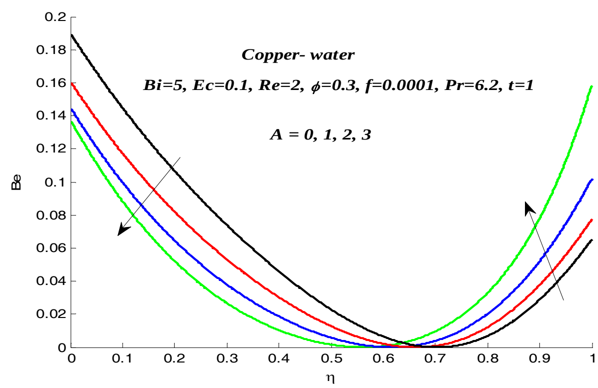

Fig. 23: Bejan number with increasing *A*

6. Conclusions

Computational model and thermodynamic analysis of the effects of Navier slip and wall permeability on entropy generation in unsteady generalized Couette flow of nanofluids containing Copper (Cu) and Alumina (Al_2O_3) as nanoparticles is presented. Using a semi-discretization method together with Runge-Kutta Fehlberg integration scheme the transient problem is numerically tackled. Some of the results obtained can be summarized as follows:

- An increase in nanoparticles volume fraction and Reynolds number causes a decrease in the velocity profile. Meanwhile nanofluid velocity profile increases with an increase in pressure gradient.
- The temperature profile increases with an increase in the nanoparticles volume fraction, slip parameter and Eckert number. But a decrease in temperature profile is noticed with an increase in Biot number.

- Skin friction increases with an increase in nanoparticles volume fraction, slip parameter and Reynolds number. But decrease with an increase in pressure gradient. The same results are obtained for the Nusselt number.
- A rise in an entropy generation rate is observed with an increase in nanoparticles volume fraction and slip parameter. It falls near the lower wall and rises near the upper wall with an increase in Biot number.
- The Bejan number increase with time at the lower and upper walls but slight decreases at the channel centreline. It increases at the walls with an increase in nanoparticles volume fraction. As Biot number and pressure gradient increases, Bejan number decreases near the lower wall and at the centre, but increases as it approaches the upper wall. Eckert number causes the increase in Bejan number at the lower and upper walls.

R F E R E N C E S

[1] *S. U. S. Choi*, Enhancing thermal conductivity of fluids with nanoparticles, In: Proc. ASME Int. Mech. Engng. Congress and Exposition, San Franciscos, USA, ASME, FED 231/MD 66, 1995, 99–105.

[2] *K. Ramakrishnan, K. Shailendhra,* Hydromagnetic Blood Flow through a Uniform Channel with Permeable Walls Covered by Porous Media of Finite, Journal of Applied Fluid Mechanics, **Vol. 6**, no. 1,2013, pp. 39-47.

[3] *O. D. Makinde, D. Theuri,* Thermodynamic analysis of variable viscosity MHD unsteady generalized Couette flow with permeable walls, Applied and Computational Mathematics, 3(1), 2014, 1-8

[4] *H. F. Oztop, E. Abu-Nada,* Numerical study of natural convection in partially heated rectangular enclosures filled with nanofluids, Int. J. Heat Fluid Flow, 29, 2008, 1326–1336.

[5] *X. Q. Wang, A. S. Mujumdar,* Heat transfer characteristics of nanofluids: a review, Int. J. Thermal Sciences, **vol. 46**, 2007, pp. 1-19.

[6] Buongiorno, J, Convective transport in nanofluids, J. Heat Transfer, **vol. 128**,2006, pp. 240-250.

[7] *R. K. Tiwari, M. K. Das,* Heat transfer augmentation in a two-sided lid-driven differentially heated square cavity utilizing nanofluids, Int. J. Heat Mass Transf., 50, 2007, 2002–2018.

[8] *A. Bejan*, Second-law analysis in heat transfer and thermal design, Adv. Heat Transfer, 15, 1982, 1–58.

[9] *A. Bejan*, Entropy Generation Minimization, CRC, Boca Raton, NY, 1996
[10] *L.C. Woods*, Thermodynamics of Fluid Systems, Oxford University Press, Oxford, 1975
[11] *U. Narusawa*, The second-law analysis of mixed convection in rectangular ducts, Heat Mass Transfer, 37, 1998, 197–203.
[12] *A. Z. Sahin*, Second law analysis of laminar viscous flow through a duct subjected to constant wall temperature, Journal of Heat Transfer, 120, 1998, 76–83.